

Uniform asymptotic expansions for Laguerre polynomials and related confluent hypergeometric functions

T. M. Dunster · A. Gil · J. Segura

Received: date / Accepted: date

Abstract Uniform asymptotic expansions involving exponential and Airy functions are obtained for Laguerre polynomials $L_n^{(\alpha)}(x)$, as well as complementary confluent hypergeometric functions. The expansions are valid for n large and α small or large, uniformly for unbounded real and complex values of x . The new expansions extend the range of computability of $L_n^{(\alpha)}(x)$ compared to previous expansions, in particular with respect to higher terms and large values of α . Numerical evidence of their accuracy for real and complex values of x is provided.

Keywords Asymptotic expansions · Laguerre polynomials · Confluent hypergeometric functions · Turning point theory, WKB methods · Numerical computation

Mathematics Subject Classification (2000) MSC 34E05 · 33C45 · 33C15 · 34E20 · 33F05

The authors acknowledge support from *Ministerio de Economía y Competitividad*, project MTM2015-67142-P (MINECO/FEDER, UE).

T. M. Dunster
Department of Mathematics and Statistics
San Diego State University. 5500 Campanile Drive San Diego, CA, USA.
E-mail: mdunster@mail.sdsu.edu

A. Gil
Departamento de Matemática Aplicada y CC. de la Computación.
ETSI Caminos. Universidad de Cantabria. 39005-Santander, Spain.
E-mail: amparo.gil@unican.es

J. Segura
Departamento de Matemáticas, Estadística y Computación.
Universidad de Cantabria. 39005-Santander, Spain.
E-mail: segura.jj@unican.es

1 Introduction

In this paper we shall obtain computable asymptotic expansions for Laguerre polynomials $L_n^{(\alpha)}(x)$, for the case n large and α small or large. These are defined by

$$L_n^{(\alpha)}(x) = \sum_{k=0}^n \binom{n+\alpha}{n-k} \frac{(-x)^k}{k!}. \quad (1.1)$$

In terms of the confluent hypergeometric functions we have

$$L_n^{(\alpha)}(x) = \frac{\Gamma(n+\alpha+1)}{n!} \mathbf{M}(-n, \alpha+1, x) = \frac{(-1)^n}{n!} U(-n, \alpha+1, x), \quad (1.2)$$

where \mathbf{M} denotes Olver's scaled confluent hypergeometric function [9, Chap. 7, sec. 9].

We will use the techniques described in [3] for computing uniform asymptotic expansions of turning point problems. These involve Airy function expansions for solutions of differential equations having a simple turning point, but in a form that differs from the classical Airy function expansions of [9, Chap. 11]. Specifically, the coefficients in these new expansions are significantly easier to compute than previously, and close to the turning point the method utilises Cauchy's integral formula. We remark that the Cauchy integral method of [3] has potential applications to other forms of differential equations, and also the method was subsequently used in [4] to compute coefficients appearing in certain asymptotic expansions of integrals.

In this paper we shall also obtain Liouville-Green (L-G) expansions for Laguerre polynomials and confluent hypergeometric functions in domains that do not contain turning points, and these involve the exponential function. The form of these expansions differs from the standard ones (see [9, Chap. 10]), inasmuch the coefficients in the expansions appear in the argument of the exponential. The advantage of this form is that the coefficients are again generally easier to compute. Indeed, L-G expansions of this form were used in [3] to obtain the new form of the Airy expansions described above.

A recent reference on the computation of Laguerre polynomials using asymptotics is [6], where three different asymptotic approximations are used: two expansions in terms of Bessel functions (from [5] and [12, Sect. 10.3.4]) and the Airy expansion of Frenzen and Wong [5]. These expansions, and in particular the Airy expansion, give accurate approximations for large n when α is not large. For large α some expansions are available, like for instance the expansions for Whittaker functions of [1] and [8], or some of the expansions in [11], but the coefficients of these expansions are very hard to compute. In this paper, we provide expansions that are computable and which can also be used for large α , and we provide numerical evidence of their accuracy for real and complex values of x .

The Laguerre polynomials satisfy the following form of the confluent hypergeometric equation

$$x \frac{d^2 y}{dx^2} + (\alpha + 1 - x) \frac{dy}{dx} + ny = 0. \quad (1.3)$$

By the transformation $\tilde{y} = x^{(\alpha+1)/2} \exp(-\frac{1}{2}x) y$ we can remove the first derivative in the usual manner, and we get

$$\frac{d^2 \tilde{y}}{dx^2} = \frac{x^2 - 2(2n + \alpha + 1)x + \alpha^2 - 1}{4x^2} \tilde{y}. \quad (1.4)$$

On replacing x by uz , where $u = n + \frac{1}{2}$ (a choice being explained after (2.9) below), this can then be re-written in the form

$$\frac{d^2 w}{dz^2} = \{u^2 f(a, z) + g(z)\} w, \quad (1.5)$$

with a solution $w = z^{(\alpha+1)/2} \exp(-\frac{1}{2}uz) L_n^{(\alpha)}(uz)$. On defining a by

$$\alpha = u(a^2 - 1) \quad (a \geq 0), \quad (1.6)$$

we have in (1.5)

$$f(z) = \frac{(z - z_1)(z - z_2)}{4z^2}, \quad g(z) = -\frac{1}{4z^2}, \quad (1.7)$$

where

$$z_1 = (a - 1)^2, \quad z_2 = (a + 1)^2. \quad (1.8)$$

The latter are the turning points for large u , which is assumed here. These turning points coalesce with each other when $a = 0$ ($\alpha = -u$), and z_1 coalesces with the pole at $z = 0$ when $a = 1$ ($\alpha = 0$).

We shall consider the following cases separately.

Case 1a: We obtain expansions for z lying in domains containing the turning point z_1 , which includes the interval $0 \leq z \leq z_2 - \delta$ (here and throughout $\delta > 0$). The turning point $z = z_2$ is excluded, and this is covered in Case 2 below. We assume $1 + \delta \leq a^2 \leq a_1 < \infty$ for fixed $a_1 \in (1, \infty)$. Thus z_1 cannot coalesce with the pole at $z = 0$ nor with the other turning point $z = z_2$, and α is positive and large, satisfying $u\delta \leq \alpha \leq u(a_1 - 1)$.

Case 1b: This is the same as Case 1a, except now we consider α negative. In particular, we assume $0 < a_0 \leq a^2 \leq 1 - \delta$ (for fixed $a_0 \in (0, 1)$), and in this case $-u(1 - a_0) \leq \alpha \leq -u\delta < 0$. Again z_1 cannot coalesce with the pole at $z = 0$ nor with the other turning point $z = z_2$.

Case 2: In this case expansions are derived for z lying in domains containing the turning point z_2 , including the interval $z_1 + \delta \leq z < \infty$, but not z_1 or 0. Here a lies in a larger interval than Cases 1a and 1b, namely $0 < a_0 \leq a^2 \leq a_1 < \infty$, and hence $-u(1 - a_0) \leq \alpha \leq u(a_1 - 1)$. Note this can include large negative values of α if $a_0 < 1$. The turning points again cannot coalesce ($a = 0$) in this case, but z_1 can coalesce with $z = 0$ (since both points are excluded).

The more general case $0 \leq a < \infty$ with $0 \leq z < \infty$ will require an application of asymptotic expansions valid for a coalescing turning point and double pole, and also for two coalescing turning points. This will be studied in a subsequent paper.

The plan of this paper is as follows. In section 2 we consider Case 1a and construct L-G expansions for the functions. In this section a detailed description of the Liouville transformation is provided. In section 3 we obtain Airy function expansions for Case 1a. In section 4 we obtain L-G and Airy expansions for Case 1b, and in section 5 we likewise do this for Case 2. Finally, in section 6 we present numerical results for the expansions of Cases 1a and 2 for Laguerre polynomials.

2 L-G expansions: Case 1a

We make the Liouville transformation

$$\xi = \int_z^{z_1} f^{1/2}(t) dt. \quad (2.1)$$

On explicit integration (and noting that $\sqrt{z_1 z_2} = |a^2 - 1|$) we obtain

$$\begin{aligned} \xi = & \frac{1}{2} (a^2 + 1) \ln \{a^2 + 1 - z - S(z)\} - \frac{1}{2} S(z) - \max \{a^2, 1\} \ln(2a) \\ & + \frac{1}{2} |a^2 - 1| \ln \left\{ \frac{(a^2 - 1)^2 + |a^2 - 1| S(z) - (a^2 + 1) z}{z} \right\}. \end{aligned} \quad (2.2)$$

In this $S(z)$ is given by

$$S(z) = \{(z_1 - z)(z_2 - z)\}^{1/2} = \left\{ z^2 - 2(a^2 + 1)z + (a^2 - 1)^2 \right\}^{1/2}, \quad (2.3)$$

where the principal logarithms are taken, and the branches of the square roots are chosen so that $S(z) > 0$ for $-\infty < z < z_1$, and is continuous elsewhere in the plane having a cut on the interval $[z_1, z_2]$. This means $S(z) < 0$ for $z_2 < z < \infty$.

Thus ξ is real and positive when $z \in (0, z_1)$, and varies continuously in the z plane having cuts along $(-\infty, 0]$ and $[z_1, \infty)$. Note that $z = z_1$ is mapped to $\xi = 0$, and $z = z_2 \pm i0$ (respectively above and below the cut) is mapped to $\xi = \pm \min \{a^2, 1\} \pi i$.

We find that $\xi \rightarrow +\infty$ as $z \rightarrow 0^+$, such that

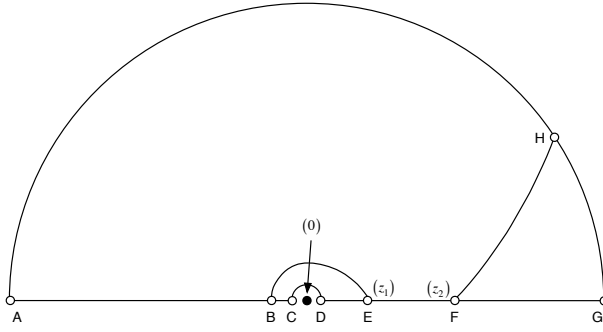
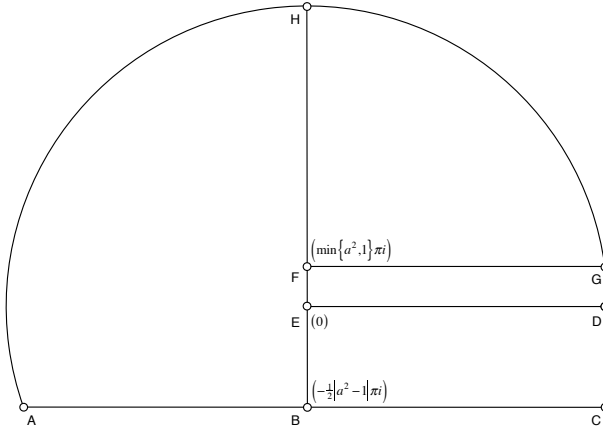
$$\xi = \frac{1}{2} |a^2 - 1| \{2 \ln |a^2 - 1| - \ln(z) - 1\} - a^2 |\ln(a)| + \mathcal{O}(z). \quad (2.4)$$

Furthermore, we have that

$$\xi = \frac{1}{2} z - \frac{1}{2} (a^2 + 1) \{\ln(z) + 1\} + a^2 \ln(a) + \min \{a^2, 1\} \pi i + \mathcal{O}(z^{-1}), \quad (2.5)$$

as $z \rightarrow \infty$ in upper half plane.

Figs. 1 and 2 depict the z - ξ map for $0 \leq \arg(z) \leq \pi$, with corresponding points labeled with the same letters. For the lower half z plane we can use from the Schwarz reflection principle that $\xi(z) = \overline{\xi(\bar{z})}$.

Fig. 1: z plane.Fig. 2: ξ plane.

With (2.1) and the new dependent variable given by

$$V = f^{1/4}(z)w, \quad (2.6)$$

the differential equation (1.5) is transformed to

$$\frac{d^2 V}{d\xi^2} = \{u^2 + \phi(\xi)\} V, \quad (2.7)$$

where

$$\begin{aligned} \phi(\xi) &= \frac{4f(z)f''(z) - 5f'^2(z)}{16f^3(z)} + \frac{g(z)}{f(z)} \\ &= -\frac{z \left\{ 4z^3 - 4(3a^2 - 1)(a^2 - 3)z + 8(a^2 + 1)(a^2 - 1)^2 \right\}}{4(z - z_1)^3(z - z_2)^3}. \end{aligned} \quad (2.8)$$

The function $\phi(\xi)$ is analytic in an unbounded domain Δ (say) which excludes $\xi = 0$ and $\xi = \pm \min\{a^2, 1\} \pi i$ (the singularities corresponding to the turning points). Then the part of Δ corresponding to $0 \leq \arg(z) \leq \pi$ is the entire region depicted in Fig. 2, except with the points $\xi = 0$ and $\xi = \min\{a^2, 1\} \pi i$ (labeled E and F, respectively) excluded.

An important property is that

$$\phi(\xi) = \mathcal{O}(\xi^{-2}), \quad (2.9)$$

as $\xi \rightarrow \infty$ in Δ . We remark that the choice of the large parameter in the form $u = n + \frac{1}{2}$, and the subsequent partitioning of (1.5), resulted in the desired behaviour (2.9).

Asymptotic solutions of (2.7), accompanied by explicit error bounds, are given in [2] by

$$V_{n,1}(u, \xi) = \exp \left\{ u\xi + \sum_{s=1}^{n-1} \frac{E_s(\xi)}{u^s} \right\} + \varepsilon_{n,1}(u, \xi), \quad (2.10)$$

and

$$V_{n,2}(u, \xi) = \exp \left\{ -u\xi + \sum_{s=1}^{n-1} (-1)^s \frac{E_s(\xi)}{u^s} \right\} + \varepsilon_{n,2}(u, \xi), \quad (2.11)$$

where the coefficients $E_s(\xi)$ will be defined below.

In (2.10) $\varepsilon_{n,1}(u, \xi) = e^{u\xi} \mathcal{O}(u^{-n})$ uniformly in a certain domain Ξ_1 , with $e^{-u\xi} \varepsilon_{n,1}(u, \xi) \rightarrow 0$ as $\operatorname{Re} \xi \rightarrow -\infty$ in the domain, and likewise in (2.11) $\varepsilon_{n,2}(u, \xi) = e^{-u\xi} \mathcal{O}(u^{-n})$ uniformly in a domain Ξ_2 , with $e^{u\xi} \varepsilon_{n,2}(u, \xi) \rightarrow 0$ as $\operatorname{Re} \xi \rightarrow \infty$ in the domain. By virtue of (2.9), both Ξ_1 and Ξ_2 are unbounded, and are defined as follows.

In general the domain of validity Ξ_1 comprises the ξ point subset of Δ for which there is a path \mathcal{P}_1 (say) linking ξ with $\alpha_1 = -\infty - \frac{1}{2}|a^2 - 1|\pi i$ (corresponding to $z = \infty e^{\pi i}$) and having the properties (i) \mathcal{P}_1 consists of a finite chain of R_2 arcs (as defined in [9, Chap. 5, sec. 3.3]), and (ii) as t passes along \mathcal{P}_1 from α_1 to ξ , $\operatorname{Re}(ut)$ is nondecreasing.

The domain Ξ_2 comprises the ξ point subset of Δ for which there is a path \mathcal{P}_2 (say) linking ξ with $\alpha_2 = +\infty$ (corresponding to $z = 0$) and having the properties (i) \mathcal{P}_2 consists of a finite chain of R_2 arcs, and (ii) as t passes along \mathcal{P}_2 from α_2 to ξ , $\operatorname{Re}(ut)$ is nonincreasing.

Let Ξ_j^+ ($j = 1, 2$) denote the subsets of Ξ_j corresponding to $0 \leq \arg(z) \leq \pi$. Then Ξ_1^+ coincides with the domain shown in Fig. 2, but with the points $\xi = 0$ and $\xi = \min\{a^2, 1\} \pi i$ excluded. We denote by D_1^+ the z -domain corresponding to Ξ_1^+ , and this is the entire upper half plane $\operatorname{Im}(z) \geq 0$ excluding the turning points $z = z_1, z_2$.

On the other hand, due to the monotonicity requirement (ii), the domain Ξ_2^+ must also exclude the unbounded region FGH of Fig. 2, as well as points on the segment EF. The corresponding z -domain D_2^+ (say) is the unshaded region depicted in Fig. 3, where the interval $[z_1, z_2]$ and the boundary curve

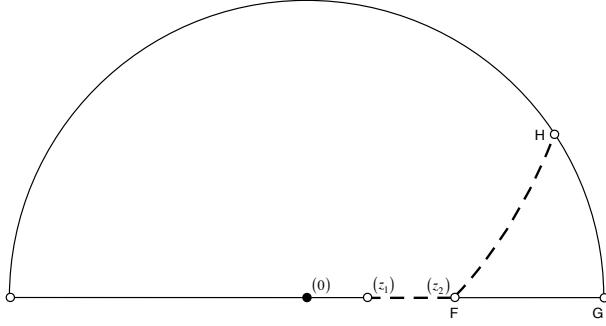


Fig. 3: Domain D_2^+ in z plane. The interval $[z_1, z_2]$ and boundary FH are excluded.

FH must be excluded; the curve FH extends from $z = z_2$ to $z = \infty$ and is given parametrically by

$$\int_{z_2}^z f^{1/2}(t) dt = \tau i, \quad 0 \leq \tau < \infty. \quad (2.12)$$

We note that $z = +\infty$ is not contained in D_2^+ (but is contained in D_1^+).

Returning to the asymptotic expansions (2.10) and (2.11), the coefficients are given by

$$E_s(\xi) = \int F_s(\xi) d\xi \quad (s = 1, 2, 3, \dots), \quad (2.13)$$

where

$$F_1(\xi) = \frac{1}{2}\phi(\xi), \quad F_2(\xi) = -\frac{1}{4}\phi(\xi), \quad (2.14)$$

and

$$F_{s+1}(\xi) = -\frac{1}{2}F'_s(\xi) - \frac{1}{2} \sum_{j=1}^{s-1} F_j(\xi) F_{s-j}(\xi) \quad (s = 2, 3, \dots). \quad (2.15)$$

Primes are derivatives with respect to ξ .

The choice of integration constants in (2.13) must be the same for both of the L-G solutions (2.10) and (2.11). As discussed in [3], the constants associated with the even terms ($s = 2j$, $j = 1, 2, 3, \dots$) are arbitrary, but those for the odd terms ($s = 2j + 1$, $j = 0, 1, 2, \dots$) must be precisely chosen, as described below.

It is preferable to work in terms of z . Using

$$\frac{d\xi}{dz} = f^{1/2}(z) = \frac{S(z)}{2z}, \quad (2.16)$$

and writing $\hat{E}_s(z) = E_s(\xi(z))$ and $\hat{F}_s(z) = F_s(\xi(z))$, we have

$$\hat{E}_s(z) = \int \frac{\hat{F}_s(z)S(z)}{2z} dz \quad (s = 1, 2, 3, \dots), \quad (2.17)$$

where

$$\hat{F}_1(z) = \frac{1}{2}\phi(\xi(z)), \quad \hat{F}_2(z) = -\frac{z}{2S(z)} \frac{d\phi(\xi(z))}{dz}, \quad (2.18)$$

and

$$\hat{F}_{s+1}(z) = -\frac{z}{S(z)} \hat{F}'_s(z) - \frac{1}{2} \sum_{j=1}^{s-1} \hat{F}_j(z) \hat{F}_{s-j}(z) \quad (s = 2, 3, \dots). \quad (2.19)$$

We find by induction that

$$\frac{\hat{F}_s(z)S(z)}{2z} = \frac{R_{2s+1}(z)}{S^{3s+2}(z)}, \quad (2.20)$$

where $R_n(z)$ is a polynomial of degree n . From this we can show that

$$\hat{E}_{2j}(z) = \frac{zT_{4j-1}^{(e)}(z)}{S^{6j}(z)}, \quad (2.21)$$

and

$$\hat{E}_{2j+1}(z) = \frac{T_{6j+3}^{(o)}(z)}{S^{6j+3}(z)}, \quad (2.22)$$

where $T_n^{(e)}(z)$ and $T_n^{(o)}(z)$ are also polynomials of degree n , provided the integration constants in (2.17) are chosen appropriately (which we assume).

For example, for the coefficient $\hat{E}_1(z)$, we have

$$\begin{aligned} T_3^{(o)}(z) = \frac{1}{48a^2} \left[(a^2 - 1)^2 \left\{ (a^2 - 1)^2 - 4a^2 \right\} - 3(a^2 + 1)^3 z \right. \\ \left. + 3(a^4 + 6a^2 + 1)z^2 - (a^2 + 1)z^3 \right]. \end{aligned} \quad (2.23)$$

We note here that $\zeta^{1/2} \hat{E}_{2j+1}(z)$, regarded as a function of $\zeta = \left(\frac{3}{2}\xi\right)^{2/3}$, is meromorphic at $\zeta = 0$. From [3] this is a requirement for the subsequent Airy function expansions to be valid at the turning point.

We also note that

$$\hat{E}_s(\infty) = \lambda_s, \quad (2.24)$$

(say), where $\lambda_{2j} = 0$ ($j = 1, 2, 3, \dots$), whereas the odd terms are non-zero. The first three of the odd terms are found to be

$$\lambda_1 = -\frac{1+a^2}{48a^2}, \lambda_3 = \frac{7(1+a^6)}{5760a^6}, \lambda_5 = -\frac{31(1+a^{10})}{80640a^{10}}. \quad (2.25)$$

We similarly find

$$\hat{E}_s(0) = \mu_s, \quad (2.26)$$

(say), where $\mu_{2j} = 0$ ($j = 1, 2, 3, \dots$), and again the odd terms are non-zero. The first two of these are found to be

$$\begin{aligned}\mu_1 &= \frac{a^4 - 6a^2 + 1}{48a^2|a^2 - 1|}, \\ \mu_3 &= -\frac{7a^{12} - 21a^{10} + 21a^8 - 30a^6 + 21a^4 - 21a^2 + 7}{5760a^6|a^2 - 1|^3}.\end{aligned}\tag{2.27}$$

Recall in this case we are assuming that $1 + \delta \leq a^2 \leq a_1 < \infty$, for fixed $a_1 \in (1, \infty)$. Thus from (1.6) α is positive, and so using

$$L_n^{(\alpha)}(x) = \frac{\Gamma(n + \alpha + 1)}{n!\Gamma(\alpha + 1)} \{1 + \mathcal{O}(x)\} \quad (x \rightarrow 0),\tag{2.28}$$

we therefore have the solution of (1.5) given by

$$w_0(u, z) \equiv z^{(\alpha+1)/2} e^{-uz/2} L_n^{(\alpha)}(uz),\tag{2.29}$$

which has the unique behaviour as $z \rightarrow 0$

$$w_0(u, z) \equiv \frac{\Gamma(n + \alpha + 1) z^{(\alpha+1)/2}}{n!\Gamma(\alpha + 1)} \{1 + \mathcal{O}(z)\}.\tag{2.30}$$

We now match solutions that are recessive at $z = 0$. From (2.6) we have by uniqueness (up to a multiplicative constant) of such solutions that

$$w_0(u, z) \propto \frac{z^{1/2} V_{n,2}(u, \xi)}{\{(z_1 - z)(z_2 - z)\}^{1/4}}.\tag{2.31}$$

Then, using (2.4), (2.11), (2.26), (2.29) and (2.30), we arrive at

$$\begin{aligned}L_n^{(\alpha)}(uz) &\sim \frac{\Gamma(n + \alpha + 1)}{n!\Gamma(\alpha + 1)} \left(\frac{\alpha}{u}\right)^{1/2} \left(\frac{u}{u + \alpha}\right)^{u/2} \left\{ \frac{\alpha^2}{(u + \alpha)uez} \right\}^{\alpha/2} \\ &\times \frac{1}{\{(z_1 - z)(z_2 - z)\}^{1/4}} \exp \left\{ \frac{1}{2}uz - u\xi + \sum_{s=1}^{\infty} (-1)^s \frac{\hat{E}_s(z) - \mu_s}{u^s} \right\}.\end{aligned}\tag{2.32}$$

This is uniformly valid for $z \in D_2^+ \cup D_2^-$, where D_2^- is the conjugate region of D_2^+ .

From [7, Eq. 13.2.24] a companion solution of (1.5) is given by

$$w_1(u, z) \equiv (uz)^{(\alpha+1)/2} e^{uz/2} U(n + \alpha + 1, \alpha + 1, uze^{-\pi i}).\tag{2.33}$$

Now from [7, Eq. 13.7.3]

$$U(n + \alpha + 1, \alpha + 1, uze^{-\pi i}) = (uze^{-\pi i})^{-n-\alpha-1} \{1 + \mathcal{O}(z^{-1})\}\tag{2.34}$$

as $z \rightarrow \infty$ for $|\arg(z e^{-\pi i})| \leq \frac{3}{2}\pi - \delta$, and we see that $w_1(u, z)$ has the behaviour

$$w_1(u, z) = (-1)^{n+1} e^{-\alpha\pi i} (uz)^{-u-\alpha/2} e^{uz/2} \{1 + \mathcal{O}(z^{-1})\},\tag{2.35}$$

and in particular this is the unique solution that is recessive in the half-plane $|\arg(ze^{-\pi i})| \leq \frac{1}{2}\pi$.

Thus we similarly deduce by matching recessive solutions that

$$w_1(u, z) \propto \frac{z^{1/2} V_{n,1}(u, \xi)}{\{(z_1 - z)(z_2 - z)\}^{1/4}}, \quad (2.36)$$

and hence using (2.5)

$$\begin{aligned} U(n + \alpha + 1, \alpha + 1, uze^{-\pi i}) &\sim -\frac{i \exp\{u + \frac{1}{2}\alpha + \max(\alpha, 0)\pi i\}}{u^{(u+1)/2}(u + \alpha)^{(u+\alpha)/2}(uz)^{\alpha/2}} \\ &\times \frac{1}{\{(z_1 - z)(z_2 - z)\}^{1/4}} \exp\left\{-\frac{1}{2}uz + u\xi + \sum_{s=1}^{\infty} \frac{\hat{E}_s(z) - \lambda_s}{u^s}\right\}. \end{aligned} \quad (2.37)$$

We remark that this expansion also holds for negative α , and in particular for $0 < a_0 \leq a^2 \leq 1 - \delta$ (for fixed $a_0 \in (0, 1)$). Likewise for its Airy expansion (3.14) below.

3 Airy expansions: Case 1a

We now obtain asymptotic expansions which are valid at $z = z_1$. These involve Airy functions, and the standard Liouville transformation is given by

$$\zeta = \left(\frac{3}{2}\xi\right)^{2/3}, \quad W = \zeta^{-1/4} f^{1/4}(z) w, \quad (3.1)$$

where ξ is again given by (2.2). Here ζ is defined to be analytic at $z = z_1$ (see [9, Chap. 11]), and moreover $\zeta > 0$ for $0 < z < z_1$, and $\zeta < 0$ for $z_1 < z < z_2$.

With this transformation the differential equation (1.5) takes the form

$$\frac{d^2 W}{d\zeta^2} = \{u^2 \zeta + \psi(\zeta)\} W, \quad (3.2)$$

where $\psi(\zeta)$ is analytic at $\zeta = 0$ (i.e. $\xi = 0$ and $z = z_1$), and is given explicitly by

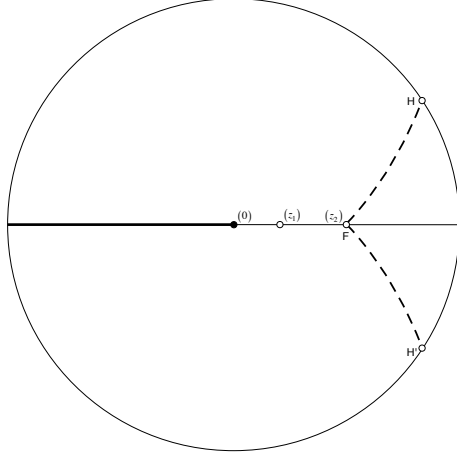
$$\psi(\zeta) = \frac{5}{16}\zeta^{-2} + \zeta\phi(\xi), \quad (3.3)$$

where $\phi(\xi)$ is given by (2.8).

From [3] the following three *exact* solutions of (3.2) are given

$$W_j(u, \zeta) = \text{Ai}_j\left(u^{2/3}\zeta\right) A(u, z) + \text{Ai}'_j\left(u^{2/3}\zeta\right) B(u, z) \quad (j = 0, \pm 1). \quad (3.4)$$

Here $\text{Ai}_j(u^{2/3}\zeta) = \text{Ai}(u^{2/3}\zeta e^{-2\pi i j/3})$, which are the Airy functions that are recessive in the sectors $\mathbf{S}_j := \{\zeta : |\arg(\zeta e^{-2\pi i j/3})| \leq \pi/3\}$; see [10, §9.2(iii)]. In our case, as functions of z , $W_0(u, \zeta)$ is recessive at $z = 0$, $W_1(u, \zeta)$ is recessive at $z = \infty e^{\pi i}$, and $W_{-1}(u, \zeta)$ is recessive at $z = \infty e^{-\pi i}$.

Fig. 4: Domain \mathbf{D} in z plane.

The coefficient functions $A(u, z)$ and $B(u, z)$ are analytic in a domain containing $z = z_1$, and in [3, Theorem 2.1] it was shown that they possess the asymptotic expansions

$$A(u, z) \sim \exp \left\{ \sum_{s=1}^{\infty} \frac{\hat{E}_{2s}(z) + \tilde{a}_{2s} \xi^{-2s}/(2s)}{u^{2s}} \right\} \times \cosh \left\{ \sum_{s=0}^{\infty} \frac{\hat{E}_{2s+1}(z) - \tilde{a}_{2s+1} \xi^{-2s-1}/(2s+1)}{u^{2s+1}} \right\}, \quad (3.5)$$

and

$$B(u, z) \sim \frac{1}{u^{1/3} \xi^{1/2}} \exp \left\{ \sum_{s=1}^{\infty} \frac{\hat{E}_{2s}(z) + a_{2s} \xi^{-2s}/(2s)}{u^{2s}} \right\} \times \sinh \left\{ \sum_{s=0}^{\infty} \frac{\hat{E}_{2s+1}(z) - a_{2s+1} \xi^{-2s-1}/(2s+1)}{u^{2s+1}} \right\}, \quad (3.6)$$

where $a_1 = a_2 = \frac{5}{72}$, $\tilde{a}_1 = \tilde{a}_2 = -\frac{7}{72}$, and for $b = a$ and $b = \tilde{a}$

$$b_{s+1} = \frac{1}{2}(s+1)b_s + \frac{1}{2} \sum_{j=1}^{s-1} b_j b_{s-j} \quad (s = 2, 3, \dots). \quad (3.7)$$

For our differential equation (3.2) these expansions are uniformly valid in an unbounded z domain \mathbf{D} , which consists of all points which can be linked to each of the singularities $z = 0, z = \infty e^{\pm \pi i}$ by a "progressive" path: that is, a finite chain of R_2 arcs that does not pass through z_2 , and with the property that $\text{Re} \xi(z)$ varies monotonically as the path is traversed from one end to the other. From Fig. 2 it is straightforward to show that \mathbf{D} consists of the

intersection of D_1^+ and D_2^+ (i.e. D_2^+ itself), along with the conjugate of D_2^+ , and in addition all points on the interval $[z_1, z_2]$.

Thus \mathbf{D} is the unshaded region shown in Fig. 4. In this $|\arg(z)| \leq \pi$, the boundary curve FH emanating from $z = z_2$ is defined by (2.12), and FH' is the conjugate curve. Points on both curves (including $z = z_2$) are excluded from \mathbf{D} , but the singularities $z = 0$ and $z = \infty e^{\pm\pi i}$ lie in \mathbf{D} , as well as of course the turning point $z = z_1$.

For each of the three solutions the respective domain of validity extends beyond \mathbf{D} . For example, for $W_0(u, \zeta)$ certain points accessible by crossing above or below the cut on the negative real axis can be included. For $W_1(u, \zeta)$ certain points crossing above this cut can be included, as well as points crossing the curve FH (but not FH'). For our purposes the common domain of validity \mathbf{D} suffices, since an extension to a domain containing $z = z_2$ and $z = +\infty$ will be considered in the next section, and for the confluent hypergeometric function analytic continuation formulas can be used for values of $\arg(z)$ outside $[-\pi, \pi]$.

We now match the Airy function expansions with the Laguerre polynomial and confluent hypergeometric function. Firstly we have, on matching the solutions recessive at $z = 0$, namely $W_0(u, \zeta)$ and $\zeta^{-1/4} f^{1/4}(z) w_0(u, z)$ (see (2.29) and (3.4)), that

$$W_0(u, \zeta) = C_0(u) \left\{ \frac{(z_1 - z)(z_2 - z)}{\zeta} \right\}^{1/4} z^{\alpha/2} e^{-uz/2} L_n^{(\alpha)}(uz), \quad (3.8)$$

for some constant $C_0(u)$.

Now as $z \rightarrow 0^+$ ($\zeta \rightarrow +\infty$) we find from (3.1), (3.5), (3.6), and the behaviour of the Airy function and its derivative for large argument (see [10, §9.7(ii)]), that the LHS behaves as

$$W_0(u, \zeta) \sim \frac{1}{2\pi^{1/2} u^{1/6} \zeta^{1/4}} \exp \left\{ -u\xi - \sum_{s=0}^{\infty} \frac{\mu_{2s+1}}{u^{2s+1}} \right\}. \quad (3.9)$$

On the other hand, from (2.28), the RHS of (3.8) has the behaviour

$$\begin{aligned} & C_0(u) \left\{ \frac{(z - z_1)(z - z_2)}{\zeta} \right\}^{1/4} z^{\alpha/2} e^{-uz/2} L_n^{(\alpha)}(uz) \\ & \sim \frac{C_0(u) \Gamma(n + \alpha + 1) (a^2 - 1)^{1/2} z^{\alpha/2}}{n! \Gamma(\alpha + 1) \zeta^{1/4}}. \end{aligned} \quad (3.10)$$

Solving for $C_0(u)$ from (3.8) - (3.10), and on referring to (1.6) and (2.5), we then arrive at

$$\begin{aligned} L_n^{(\alpha)}(uz) &\sim \frac{2\pi^{1/2}u^{1/6}\Gamma(n+\alpha+1)}{n!\Gamma(\alpha+1)} \left(\frac{\alpha}{u}\right)^{1/2} \left(\frac{u}{u+\alpha}\right)^{u/2} \\ &\times \left(\frac{\alpha^2}{(u+\alpha)uez}\right)^{\alpha/2} \left\{\frac{\zeta}{(z_1-z)(z_2-z)}\right\}^{1/4} \exp\left\{\frac{1}{2}uz + \sum_{s=0}^{\infty} \frac{\mu_{2s+1}}{u^{2s+1}}\right\} \\ &\times \left\{\text{Ai}(u^{2/3}\zeta) A(u, z) + \text{Ai}'(u^{2/3}\zeta) B(u, z)\right\}. \end{aligned} \quad (3.11)$$

Similarly, on matching solutions recessive at $z = \infty e^{\pi i}$ we assert the existence of a constant $C_1(u)$ such that

$$\begin{aligned} W_1(u, \zeta) &= C_1(u) \left\{\frac{(z_1-z)(z_2-z)}{\zeta}\right\}^{1/4} \\ &\times z^{\alpha/2} e^{uz/2} U(n+\alpha+1, \alpha+1, uze^{-\pi i}). \end{aligned} \quad (3.12)$$

The constant is found by comparing both sides as $z \rightarrow \infty e^{\pi i}$, and as a result, on using

$$\begin{aligned} &\text{Ai}_1(u^{2/3}\zeta) A(u, z) + \text{Ai}'_1(u^{2/3}\zeta) B(u, z) \\ &\sim \frac{e^{\pi i/6}}{2\pi^{1/2}u^{1/6}\zeta^{1/4}} \exp\left\{u\xi + \sum_{s=0}^{\infty} \frac{\lambda_{2s+1}}{u^{2s+1}}\right\}, \end{aligned} \quad (3.13)$$

we find that

$$\begin{aligned} &U(n+\alpha+1, \alpha+1, uze^{-\pi i}) \\ &\sim -\frac{2\pi^{1/2}e^{\pi i/3}}{u^{1/3}\{u(u+\alpha)\}^{(u+\alpha)/2} z^{\alpha/2}} \left\{\frac{\zeta}{(z_1-z)(z_2-z)}\right\}^{1/4} \\ &\times \exp\left\{-\frac{1}{2}uz + u + \frac{1}{2}\alpha + \max(\alpha, 0)\pi i - \sum_{s=0}^{\infty} \frac{\lambda_{2s+1}}{u^{2s+1}}\right\} \\ &\times \left\{\text{Ai}_1(u^{2/3}\zeta) A(u, z) + \text{Ai}'_1(u^{2/3}\zeta) B(u, z)\right\}. \end{aligned} \quad (3.14)$$

By the matching of solutions that are recessive as $z \rightarrow \infty e^{-\pi i}$, we obtain corresponding L-G and Airy asymptotic expansions which are given by (2.37) and (3.14) respectively, with i replaced by $-i$ in both, and Ai_1 replaced by Ai_{-1} in the latter. Likewise for (5.18) and (5.20) below.

4 L-G and Airy expansions: Case 1b

Now let us consider the case $0 < a_0 \leq a^2 \leq 1 - \delta$ ($-u(1-a_0) \leq \alpha \leq -u\delta < 0$). As mentioned earlier, in this case the expansions (2.37) and (3.14) remain valid for $U(n+\alpha+1, \alpha+1, uze^{-\pi i})$. However, the same is not true for

the corresponding expansions (2.32) and (3.11) of $L_n^{(\alpha)}(uz)$. This is because $w_0(u, z)$ (defined by (2.29)) is in general not recessive at $z = 0$ when $\alpha < 0$ (except when α is an integer). Indeed, this time the appropriate solution recessive at the origin is given by

$$w_2(u, z) \equiv z^{(\alpha+1)/2} e^{-uz/2} \mathbf{N}(-n, \alpha + 1, uz), \quad (4.1)$$

where $\mathbf{N}(a, c, x)$ is Olver's scaled confluent hypergeometric function defined in [9, Chap. 7, sec. 9]. In particular we have for $\alpha \neq 1, 2, 3, \dots$

$$\mathbf{N}(-n, \alpha + 1, x) = \frac{x^{-\alpha}}{\Gamma(1 - \alpha)} \{1 + \mathcal{O}(x)\} \quad (x \rightarrow 0), \quad (4.2)$$

and hence

$$w_2(u, z) \equiv \frac{z^{(1-\alpha)/2}}{\Gamma(1 - \alpha) u^\alpha} \{1 + \mathcal{O}(z)\} \quad (z \rightarrow 0). \quad (4.3)$$

Comparing this to (2.30) we see that $w_2(u, z)$ has the desired recessive behaviour at $z = 0$ when $\alpha < 0$. We remark that when α is a negative integer $w_0(u, z)$ and $w_2(u, z)$ are multiples of one another, since if $\alpha = -p$ for any integer $p \in [1, n]$ we have from (1.1) and (2.29)

$$w_0(u, z) = \frac{(-u)^p z^{(p+1)/2}}{p!} \{1 + \mathcal{O}(z)\} \quad (z \rightarrow 0). \quad (4.4)$$

By identifying $w_2(u, z)$ and $f^{-1/4}(z) V_{n,2}(u, \xi)$ in a similar manner to (2.31), we find for $-u(1 - a_0) \leq \alpha \leq -u\delta < 0$ that

$$\begin{aligned} \mathbf{N}(-n, \alpha + 1, uz) &\sim \frac{1}{\Gamma(1 - \alpha)} \left(\frac{|\alpha|}{u}\right)^{1/2} \left(\frac{u + \alpha}{u}\right)^{u/2} \left\{\frac{(u + \alpha)e}{\alpha^2 uz}\right\}^{\alpha/2} \\ &\times \frac{1}{\{(z_1 - z)(z_2 - z)\}^{1/4}} \exp\left\{\frac{1}{2}uz - u\xi + \sum_{s=1}^{\infty} (-1)^s \frac{\hat{E}_s(z) - \mu_s}{u^s}\right\}, \end{aligned} \quad (4.5)$$

uniformly for $z \in D_2^+ \cup D_2^-$.

Likewise, analogously to (3.11)

$$\begin{aligned} \mathbf{N}(-n, \alpha + 1, uz) &\sim \frac{2\pi^{1/2} u^{1/6}}{\Gamma(1 - \alpha)} \left(\frac{|\alpha|}{u}\right)^{1/2} \left(\frac{u + \alpha}{u}\right)^{u/2} \\ &\times \left\{\frac{(u + \alpha)e}{\alpha^2 uz}\right\}^{\alpha/2} \left\{\frac{\zeta}{(z_1 - z)(z_2 - z)}\right\}^{1/4} \exp\left\{\frac{1}{2}uz + \sum_{s=0}^{\infty} \frac{\mu_{2s+1}}{u^{2s+1}}\right\} \\ &\times \{\text{Ai}(u^{2/3}\zeta) A(u, z) + \text{Ai}'(u^{2/3}\zeta) B(u, z)\}, \end{aligned} \quad (4.6)$$

uniformly for $z \in \mathbf{D}$.

To obtain the desired expansions for the Laguerre polynomials we use (1.2) and the connection formula

$$\begin{aligned} \mathbf{M}(-n, \alpha + 1, z) &= \frac{e^{\alpha\pi i} n!}{\Gamma(n + \alpha + 1)} \mathbf{N}(-n, \alpha + 1, z) \\ &\quad - \frac{\sin(\pi\alpha) n!}{\pi} e^z U(n + \alpha + 1, \alpha + 1, ze^{-\pi i}), \end{aligned} \quad (4.7)$$

to obtain

$$\begin{aligned} L_n^{(\alpha)}(uz) &= e^{\alpha\pi i} \mathbf{N}(-n, \alpha + 1, z) \\ &\quad - \pi^{-1} \sin(\pi\alpha) \Gamma(n + \alpha + 1) e^z U(n + \alpha + 1, \alpha + 1, ze^{-\pi i}). \end{aligned} \quad (4.8)$$

On inserting the expansions (2.37) and (4.5) into (4.8) yields the desired L-G expansion for $L_n^{(\alpha)}(uz)$ for $-u(1 - a_0) \leq \alpha \leq -u\delta < 0$. Likewise, the corresponding Airy expansion comes from (3.14), (4.6), and (4.8).

5 L-G and Airy expansions: Case 2

We note that $S(z) < 0$ for $z \in (z_2, \infty)$, where $S(z)$ is given by (2.3). Hence the same is true for $f^{1/2}(z) = S(z)/(2z)$, and with this in mind we now define the L-G variable by

$$\tilde{\xi} = - \int_{z_2}^z f^{1/2}(t) dt, \quad (5.1)$$

so that $\tilde{\xi} \geq 0$ for $z \geq z_2$. Explicit integration yields

$$\begin{aligned} \tilde{\xi} &= -\frac{1}{2}(a^2 + 1) \ln \{z - S(z) - a^2 - 1\} - \frac{1}{2}S(z) + \max\{a^2, 1\} \ln(2a) \\ &\quad - \frac{1}{2}|a^2 - 1| \ln \left\{ \frac{(a^2 + 1)z - (a^2 - 1)^2 + |a^2 - 1|S(z)}{z} \right\}. \end{aligned} \quad (5.2)$$

We observe that $\tilde{\xi} = \xi - \min\{a^2, 1\} \pi i$, where ξ is the corresponding L-G variable from case 1.

The L-G asymptotic solution that we employ this time is given by the expansion

$$\tilde{V}_{n,2}(u, \tilde{\xi}) = \exp \left\{ -u\tilde{\xi} + \sum_{s=1}^{n-1} (-1)^s \frac{\hat{E}_s(z)}{u^s} \right\} + \tilde{\varepsilon}_{n,2}(u, \tilde{\xi}), \quad (5.3)$$

where the coefficients $\hat{E}_s(z)$ are the same as in Cases 1a and 1b.

In (5.3) $\tilde{\varepsilon}_{n,2}(u, \tilde{\xi}) = e^{-u\tilde{\xi}} \mathcal{O}(u^{-n})$ uniformly in a certain unbounded domain $\tilde{\Xi}_2$, with $e^{u\tilde{\xi}} \tilde{\varepsilon}_{n,2}(u, \tilde{\xi}) \rightarrow 0$ as $\text{Re } \tilde{\xi} \rightarrow \infty$ in the domain. Let $\tilde{\Delta}$ denote the domain in the $\tilde{\xi}$ plane corresponding to Δ in the ξ plane: thus it is Δ

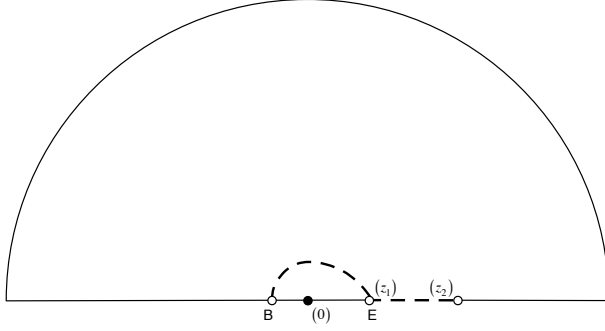


Fig. 5: Domain \tilde{D}_2^+ in z plane. The interval $[z_1, z_2]$ and boundary EB are excluded.

shifted by the factor $-\min\{a^2, 1\}\pi i$. Then the domain $\tilde{\Xi}_2$ comprises the $\tilde{\xi}$ point subset of $\tilde{\Delta}$ for which there is a path $\tilde{\mathcal{P}}_2$ (say) linking $\tilde{\xi}$ with $\tilde{\alpha}_2 = +\infty$ (corresponding to $z = +\infty + i0$) and having the properties (i) $\tilde{\mathcal{P}}_2$ consists of a finite chain of R_2 arcs, and (ii) as t passes along $\tilde{\mathcal{P}}_2$ from $\tilde{\alpha}_2$ to $\tilde{\xi}$, $\text{Re}(ut)$ is nonincreasing.

If $\tilde{\Xi}_2^+$ denotes the subset of $\tilde{\Xi}_2$ corresponding to $0 \leq \arg(z) \leq \pi$, then due to condition (ii) above $\tilde{\Xi}_2^+$ must also exclude all points in the fourth quadrant of the $\tilde{\xi}$ plane. The corresponding z -domain \tilde{D}_2^+ (say) is thus unshaded region depicted in Fig. 5, where the interval $[z_1, z_2]$ and the boundary curve EB must be excluded; the curve EB emanates from $z = z_1$ to a point on the upper part of the cut along $(-\infty, 0)$, and is given parametrically by

$$\int_{z_1}^z f^{1/2}(t) dt = -\tau i, \quad 0 \leq \tau \leq \frac{1}{2}|a^2 - 1|. \quad (5.4)$$

We remark that $z = 0$ is not contained in \tilde{D}_2^+ .

We now use the behaviour of the Laguerre polynomials at infinity to match it with the L-G expansion (5.3). Specifically, we know that

$$L_n^{(\alpha)}(uz) = \frac{(-1)^n}{n!} U(-n, \alpha + 1, uz), \quad (5.5)$$

and hence the following solution of (1.5)

$$\tilde{w}_0(u, z) \equiv (uz)^{(\alpha+1)/2} e^{-uz/2} L_n^{(\alpha)}(uz), \quad (5.6)$$

has, from [7, Eq. 13.7.3], the behaviour as $z \rightarrow \infty$

$$\tilde{w}_0(u, z) = \frac{(-1)^n}{n!} (uz)^{(2u+\alpha)/2} e^{-uz/2} \left\{ 1 + \mathcal{O}\left(\frac{1}{z}\right) \right\}. \quad (5.7)$$

On comparing this to (2.35) we see that $\tilde{w}_0(u, z)$ is the unique solution that is recessive in right half plane. On matching, we therefore ascertain that there exists a constant $\tilde{c}_0(u)$ such that

$$\tilde{w}_0(u, z) = \tilde{c}_0(u) f^{-1/4}(z) \tilde{V}_{n,2}\left(u, \tilde{\xi}\right), \quad (5.8)$$

where $\tilde{V}_{n,2}\left(u, \tilde{\xi}\right)$ is given by (5.3).

Using

$$\tilde{\xi} = \frac{1}{2}z - \frac{1}{2}(a^2 + 1)\{\ln(z) + 1\} + a^2 \ln(a) + \mathcal{O}(z^{-1}) \quad (z \rightarrow \infty), \quad (5.9)$$

we have from (5.3), (2.24) and (5.7)

$$\begin{aligned} \tilde{c}_0(u) &= \lim_{z \rightarrow \infty} \left\{ \frac{f^{1/4}(z) \tilde{w}_0(u, z)}{\tilde{V}_{n,2}\left(u, \tilde{\xi}\right)} \right\} \\ &\sim \frac{(-1)^n u^{u/2} (u + \alpha)^{(u+\alpha)/2}}{\sqrt{2} e^{u+(\alpha/2)n} n!} \exp \left\{ - \sum_{s=1}^{\infty} (-1)^s \frac{\lambda_s}{u^s} \right\}. \end{aligned} \quad (5.10)$$

Hence from (5.6), (5.8) and (5.10)

$$\begin{aligned} L_n^{(\alpha)}(uz) &\sim \frac{(-1)^n u^{(u-1)/2} (u + \alpha)^{(u+\alpha)/2}}{e^{u+(\alpha/2)n} n! (uz)^{\alpha/2} \{(z - z_1)(z - z_2)\}^{1/4}} \\ &\times \exp \left\{ \frac{1}{2}uz - u\tilde{\xi} + \sum_{s=1}^{\infty} (-1)^s \frac{\hat{E}_s(z) - \lambda_s}{u^s} \right\}, \end{aligned} \quad (5.11)$$

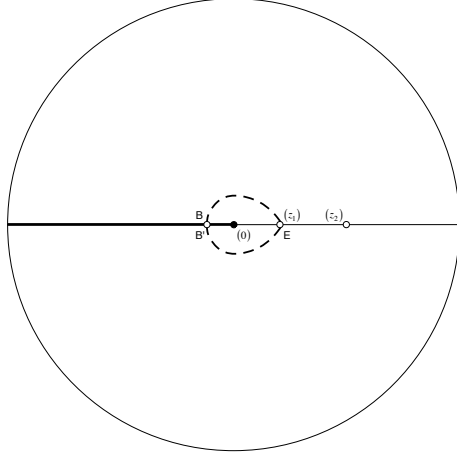
uniformly for $z \in \tilde{D}_2^+ \cup \tilde{D}_2^-$, where \tilde{D}_2^- is the conjugate region of \tilde{D}_2^+ . We emphasise that this expansion is not valid on the interval $[z_1, z_2]$.

We next construct an Airy function expansion, which is valid at $z = z_2$, similarly to (3.11). We have, again by matching solutions (3.4) with $j = 0$ (all recessive at $z = +\infty$) with (5.6), that

$$\begin{aligned} \tilde{C}_0(u) &\left\{ \frac{(z - z_1)(z - z_2)}{\tilde{\zeta}} \right\}^{1/4} z^{\alpha/2} e^{-uz/2} L_n^{(\alpha)}(uz) \\ &= \text{Ai} \left(u^{2/3} \tilde{\zeta} \right) \tilde{A}(u, z) + \text{Ai}' \left(u^{2/3} \tilde{\zeta} \right) \tilde{B}(u, z), \end{aligned} \quad (5.12)$$

for some constant $\tilde{C}_0(u)$. Here $\tilde{\zeta} = \left(\frac{3}{2} \tilde{\xi} \right)^{2/3}$, where $\tilde{\xi}$ is given by (5.2), and the coefficient functions $\tilde{A}(u, z)$ and $\tilde{B}(u, z)$ are analytic at $z = z_2$ ($\tilde{\zeta} = 0$). These have the expansions (c.f. (3.5) and (3.6))

$$\begin{aligned} \tilde{A}(u, z) &\sim \exp \left\{ \sum_{s=1}^{\infty} \frac{\hat{E}_{2s}(z) + \tilde{a}_{2s} \tilde{\xi}^{-2s} / (2s)}{u^{2s}} \right\} \\ &\times \cosh \left\{ \sum_{s=0}^{\infty} \frac{\hat{E}_{2s+1}(z) - \tilde{a}_{2s+1} \tilde{\xi}^{-2s-1} / (2s+1)}{u^{2s+1}} \right\}, \end{aligned} \quad (5.13)$$

Fig. 6: Domain $\tilde{\mathbf{D}}$ in z plane.

and

$$\begin{aligned} \tilde{B}(u, z) &\sim \frac{1}{u^{1/3}\tilde{\zeta}^{1/2}} \exp \left\{ \sum_{s=1}^{\infty} \frac{\hat{E}_{2s}(z) + a_{2s}\tilde{\xi}^{-2s}/(2s)}{u^{2s}} \right\} \\ &\times \sinh \left\{ \sum_{s=0}^{\infty} \frac{\hat{E}_{2s+1}(z) - a_{2s+1}\tilde{\xi}^{-2s-1}/(2s+1)}{u^{2s+1}} \right\}. \end{aligned} \quad (5.14)$$

uniformly for $z \in \tilde{\mathbf{D}}$; this domain is the unshaded region depicted in Fig. 6, where EB' is the conjugate curve of EB . All points on the boundary curve $B'EB$ are excluded from $\tilde{\mathbf{D}}$.

Now as $\tilde{\zeta} \rightarrow \infty$ we find from (5.13), (5.14), and the behaviour of the Airy function and its derivative for large argument [10, §9.7(ii)], that the RHS behaves as

$$\begin{aligned} &\text{Ai}(u^{2/3}\tilde{\zeta}) \tilde{A}(u, z) + \text{Ai}'(u^{2/3}\tilde{\zeta}) \tilde{B}(u, z) \\ &\sim \frac{1}{2\pi^{1/2}u^{1/6}\tilde{\zeta}^{1/4}} \exp \left\{ -u\tilde{\zeta} - \sum_{s=0}^{\infty} \frac{\lambda_{2s+1}}{u^{2s+1}} \right\}. \end{aligned} \quad (5.15)$$

On the other hand, from (5.7), the LHS has the behaviour

$$\begin{aligned} &\tilde{C}_0(u) \left\{ \frac{(z - z_1)(z - z_2)}{\tilde{\zeta}} \right\}^{1/4} z^{\alpha/2} e^{-uz/2} L_n^{(\alpha)}(uz) \\ &\sim \frac{(-1)^n \tilde{C}_0(u) u^n z^{(2n+\alpha+1)/2} e^{-uz/2}}{n! \tilde{\zeta}^{1/4}}. \end{aligned} \quad (5.16)$$

Thus from (1.6), (5.9), (5.12) - (5.16) we can solve for $\tilde{C}_0(u)$, and from this deduce that

$$\begin{aligned} L_n^{(\alpha)}(uz) &\sim \frac{(-1)^n 2\pi^{1/2} u^{(u/2)-(1/3)} (u+\alpha)^{(u+\alpha)/2}}{n! (uz)^{\alpha/2}} \\ &\times \left\{ \frac{\tilde{\zeta}}{(z-z_1)(z-z_2)} \right\}^{1/4} \exp \left\{ \frac{1}{2}uz - u - \frac{1}{2}\alpha + \sum_{s=0}^{\infty} \frac{\lambda_{2s+1}}{u^{2s+1}} \right\} \\ &\times \left\{ \text{Ai} \left(u^{2/3} \tilde{\zeta} \right) \tilde{A}(u, z) + \text{Ai}' \left(u^{2/3} \tilde{\zeta} \right) \tilde{B}(u, z) \right\}. \end{aligned} \quad (5.17)$$

For the complementary solution we have, equivalent to (2.37), the asymptotic expansion

$$\begin{aligned} U(n+\alpha+1, \alpha+1, uze^{-\pi i}) &\sim \frac{(-1)^{n+1} e^{\alpha\pi i + u + (\alpha/2)}}{u^{(u+1)/2} (u+\alpha)^{(u+\alpha)/2}} \\ &\times \frac{1}{(uz)^{\alpha/2} \{(z-z_1)(z-z_2)\}^{1/4}} \\ &\times \exp \left\{ -\frac{1}{2}uz + u\tilde{\xi} + \sum_{s=1}^{\infty} \frac{\hat{E}_s(z) - \lambda_s}{u^s} \right\}. \end{aligned} \quad (5.18)$$

Similarly to the derivation of (5.17), using

$$\begin{aligned} &\text{Ai}_1 \left(u^{2/3} \tilde{\zeta} \right) \tilde{A}(u, z) + \text{Ai}'_1 \left(u^{2/3} \tilde{\zeta} \right) \tilde{B}(u, z) \\ &\sim \frac{e^{\pi i/6}}{2\pi^{1/2} u^{1/6} \tilde{\zeta}^{1/4}} \exp \left\{ u\tilde{\xi} + \sum_{s=0}^{\infty} \frac{\lambda_{2s+1}}{u^{2s+1}} \right\}, \end{aligned} \quad (5.19)$$

we arrive at

$$\begin{aligned} U(n+\alpha+1, \alpha+1, uze^{-\pi i}) &\sim \frac{(-1)^{n+1} 2\pi^{1/2} e^{-\pi i/6} e^{\alpha\pi i}}{u^{1/3} \{u(u+\alpha)\}^{(u+\alpha)/2} z^{\alpha/2}} \\ &\times \left\{ \frac{\tilde{\zeta}}{(z-z_1)(z-z_2)} \right\}^{1/4} \exp \left\{ -\frac{1}{2}uz + u + \frac{1}{2}\alpha - \sum_{s=0}^{\infty} \frac{\lambda_{2s+1}}{u^{2s+1}} \right\} \\ &\times \left\{ \text{Ai}_1 \left(u^{2/3} \tilde{\zeta} \right) \tilde{A}(u, z) + \text{Ai}'_1 \left(u^{2/3} \tilde{\zeta} \right) \tilde{B}(u, z) \right\}. \end{aligned} \quad (5.20)$$

6 Numerical results

Here we illustrate the accuracy of the new expansions for Cases 1a and 2. We concentrate on Laguerre polynomials with n large and α non-negative, but analogous results are available for negative α , as well as for the complementary confluent hypergeometric functions.

6.1 Case 1a

In this case the expansions are valid in domains containing $z = 0$ and $z = z_1$. The relevant L-G expansion is given by (2.32), and after truncating after $N \geq 1$ terms we have

$$\begin{aligned} L_n^{(\alpha)}(uz) &= \frac{\Gamma(n + \alpha + 1)}{n! \Gamma(\alpha + 1)} \left(\frac{\alpha}{u}\right)^{1/2} \left(\frac{u}{u + \alpha}\right)^{u/2} \\ &\times \left\{ \frac{\alpha^2}{(u + \alpha)uez} \right\}^{\alpha/2} \frac{1}{\{(z_1 - z)(z_2 - z)\}^{1/4}} \\ &\times \exp \left\{ \frac{1}{2}uz - u\xi + \sum_{s=1}^N (-1)^s \frac{\hat{E}_s(z) - \mu_s}{u^s} \right\} \left\{ 1 + \mathcal{O}\left(\frac{1}{u^{N+1}}\right) \right\}. \end{aligned} \quad (6.1)$$

The order term is uniformly valid for $z \in D_2^+ \cup D_2^-$, where D_2^+ is shown in Fig. 3, and D_2^- is the conjugate region of D_2^+ .

The Airy expansion is given by (3.11), and (3.5) and (3.6) are used to approximate the coefficient functions. Therefore uniformly for $z \in \mathbf{D}$ (the domain of validity depicted in Fig. 4) we have

$$\begin{aligned} L_n^{(\alpha)}(uz) &= \frac{2\pi^{1/2}u^{1/6}\Gamma(n + \alpha + 1)}{n! \Gamma(\alpha + 1)} \left(\frac{\alpha}{u}\right)^{1/2} \left(\frac{u}{u + \alpha}\right)^{u/2} \\ &\times \left(\frac{\alpha^2}{(u + \alpha)uez}\right)^{\alpha/2} \exp \left\{ \frac{1}{2}uz + \sum_{s=0}^{m-1} \frac{\mu_{2s+1}}{u^{2s+1}} \right\} \\ &\times \left[\text{Ai}(u^{2/3}\zeta) \left\{ \mathcal{A}_m(u, z) + \mathcal{O}\left(\frac{1}{u^{2m+1}}\right) \right\} \right. \\ &\left. + \text{Ai}'(u^{2/3}\zeta) \left\{ \mathcal{B}_m(u, z) + \mathcal{O}\left(\frac{1}{u^{2m+4/3}}\right) \right\} \right]. \end{aligned} \quad (6.2)$$

In this, for any positive integer m , we have introduced the truncated expansions

$$\begin{aligned} \mathcal{A}_m(u, z) &= \chi(u, z) \exp \left\{ \sum_{s=1}^m \frac{\hat{E}_{2s}(z) + \tilde{a}_{2s}\xi^{-2s}/(2s)}{u^{2s}} \right\} \\ &\times \cosh \left\{ \sum_{s=0}^{m-1} \frac{\hat{E}_{2s+1}(z) - \tilde{a}_{2s+1}\xi^{-2s-1}/(2s+1)}{u^{2s+1}} \right\}, \end{aligned} \quad (6.3)$$

and

$$\begin{aligned} \mathcal{B}_m(u, z) &= \frac{\chi(u, z)}{u^{1/3}\zeta^{1/2}} \exp \left\{ \sum_{s=1}^m \frac{\hat{E}_{2s}(z) + a_{2s}\xi^{-2s}/(2s)}{u^{2s}} \right\} \\ &\times \sinh \left\{ \sum_{s=0}^{m-1} \frac{\hat{E}_{2s+1}(z) - a_{2s+1}\xi^{-2s-1}/(2s+1)}{u^{2s+1}} \right\}, \end{aligned} \quad (6.4)$$

where

$$\chi(u, z) = \left\{ \frac{\zeta}{(z_1 - z)(z_2 - z)} \right\}^{1/4}. \quad (6.5)$$

We remark that the term $\chi(u, z)$ has been absorbed into the scaled functions $\mathcal{A}_m(u, z)$ and $\mathcal{B}_m(u, z)$ because it has a removable singularity at $z = z_1$ ($\zeta = 0$), and hence it is easier to compute via Cauchy's integral formula when z is close to z_1 , as described next.

Let $z \in \mathbf{D}$: if this point is not too close to the turning point z_1 we can use (6.3) and (6.4) directly for their numerically stable computation in (6.2). On the other hand, if z is close to z_1 these expansions are not stable, since each $\hat{E}_s(z)$ is unbounded at this turning point. Instead we follow [3] to compute these functions via Cauchy's integral formula. Now, neither $\mathcal{A}_m(u, z)$ nor $\mathcal{B}_m(u, z)$ are analytic at $z = z_1$, but $\chi(u, z)A(u, z)$ and $\chi(u, z)B(u, z)$ are. Thus, we have

$$\begin{aligned}\chi(u, z)A(u, z) &= \frac{1}{2\pi i} \oint_{\mathcal{L}_1} \frac{\chi(u, t)A(u, t)}{t - z} dt \\ &= \frac{1}{2\pi i} \oint_{\mathcal{L}_1} \frac{\mathcal{A}_m(u, t) + \mathcal{O}(u^{-2m-1})}{t - z} dt \\ &= \frac{1}{2\pi i} \oint_{\mathcal{L}_1} \frac{\mathcal{A}_m(u, t)}{t - z} dt + \mathcal{O}\left(\frac{1}{u^{2m+1}}\right),\end{aligned}\tag{6.6}$$

for some suitably-chosen bounded simple loop \mathcal{L}_1 in the t -plane that is positively orientated, lies in an equivalent domain to \mathbf{D} , and surrounds $t = z$ and $t = z_1$. Hence in (6.2) it is legitimate (if necessary) to replace $\mathcal{A}_m(u, z)$ by $(2\pi i)^{-1} \oint_{\mathcal{L}_1} \mathcal{A}_m(u, t)(t - z)^{-1} dt$, and similarly for $\mathcal{B}_m(u, z)$. We then compute these integrals using the trapezoidal rule, which has exponential convergence.

In our computations we shall take N even and $m = N/2$ so that the order terms in (6.1) and (6.2) are of comparable magnitude (and likewise for Case 2 considered later). Note that for fixed ζ

$$\begin{aligned}u^{1/6}\text{Ai}(u^{2/3}\zeta) &= \exp(-u\xi)\mathcal{O}(1), \\ u^{1/6}\text{Ai}'(u^{2/3}\zeta) &= \exp(-u\xi)\mathcal{O}(u^{1/3}),\end{aligned}\tag{6.7}$$

as $u \rightarrow \infty$ (see [10, §9.7(ii)]).

If we consider the natural choice of \mathcal{L}_1 being a circular path centred on z_1 , it should have a radius smaller than

$$r_m = \min\{z_1, z_2 - z_1\}.\tag{6.8}$$

We have that $r_m = z_1$ when $a \leq 3 + 2\sqrt{2}$ (that is, $\alpha/(n + 1/2) \leq 4(4 + 3\sqrt{2})$) and $r_m = z_2 - z_1$ if $a \geq 3 + 2\sqrt{2}$. When we have to use Cauchy's integral formula (for z close to z_1) it is clear that $\text{Re } z > 0$; however, we have shown that the validity of both the L-G approximation and the Airy expansion away from the turning point z_1 extends to $\text{Re } z < 0$. We first consider circular \mathcal{L}_1 as described above with a radius smaller than r_m , and later we give details

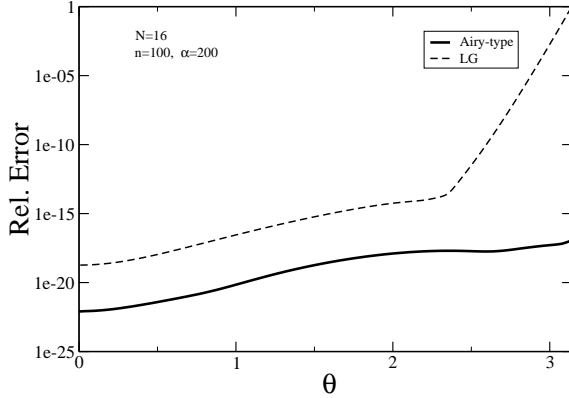


Fig. 7: Relative errors ϵ_{rel} for the L-G expansion (6.1) and the Airy expansion (6.2), with coefficients computed from (6.3) and (6.4), as a function of θ , where $z = z_1 - Re^{-i\theta}$, $\theta \in [0, \pi]$ and $R = 0.5r_m = 0.5z_1$.

for $\text{Re } z < 0$ where we can use (6.3) and (6.4) directly (without resorting to Cauchy integrals).

Let the relative error of an approximation f^* of a function f be defined in the usual manner by

$$\epsilon_{rel} = \left| \frac{f - f^*}{f} \right|. \quad (6.9)$$

Then in Fig. 7 we show the relative errors of the L-G expansion (6.1) and the Airy expansion (6.2) for the Laguerre polynomial. In both cases ϵ_{rel} is shown as a function of the angle when the upper half circle centered at z_1 is followed clockwise. As expected, we observe a step increase in the relative error for the L-G approximation as we cross a Stokes line; contrarily, the Airy expansion works well for all angles. In addition, we observe that the relative error for the Airy expansion is smaller than for the L-G expansion for all θ . Fig. 8 also shows that this is true for real values $0 < z < z_1$, while for negative z both expansions give similar accuracies.

In these and in most of the figures, we consider the case of Laguerre polynomials of degree $n = 100$ and we use (6.1) with $N = 16$ and (6.3) and (6.4) with $m = 8$. If a higher degree n or a larger number of coefficients is considered, the accuracy will improve (except, of course, if N or m is too large, because the series are asymptotic but not convergent).

Fig. 9 shows the maximum relative error over circles centred at z_1 of different radii (but always contained in the strip $\{z : 0 < \text{Re } z < z_2\}$). For the curves corresponding to $a < 3 + 2\sqrt{2}$ ($\alpha = 100, 1000$) the circles do not get close to z_2 , and this is why the relative error is monotonic as r increases. In the other to cases, the circle touches z_2 when $r = 1$ which explains the different

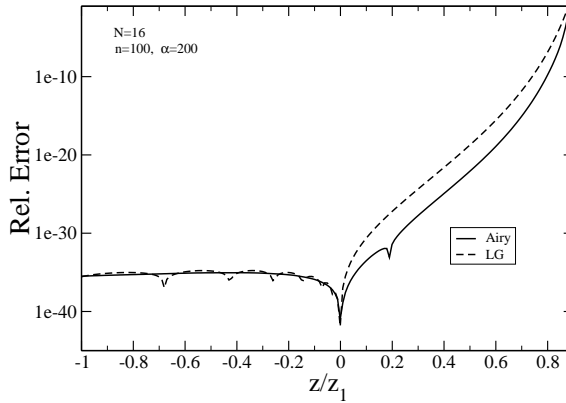


Fig. 8: Relative errors ϵ_{rel} for the L-G expansion (6.1) and the Airy expansion (6.2), with coefficients computed from (6.3) and (6.4), as a function of z/z_1 for real values of z , $z < z_1$.

pattern. We observe that the approximation works for α large comparable to n but that when α is too large accuracy is lost.

The circles considered in Fig. 9 are the only circles centered at z_1 that can be used for computing the coefficients of the Airy expansion by Cauchy integrals. Indeed, we can not consider $z > z_2$ because the expansions are meaningless there, and we can not consider $\text{Re } z < 0$ because of the discontinuity branch at the negative real axis (which implies a discontinuity in the coefficients $A(u, z)$ and $B(u, z)$).

However, as commented earlier and shown in Fig. 8, the Airy expansion (with coefficients computed by L-G asymptotics) is valid for $\text{Re } z < 0$. In particular it is also valid for negative z , as Fig. 10 also shows. In this figure, we plot the relative error of the Airy expansion (with coefficients from asymptotics) for real z as a function of $\tau = (z - z_1) / (z_2 - z_1)$. This plot includes negative values of z for the two smaller values of α , for $\tau < \tau(0) \approx -0.0301$ when $\alpha = 100$ and for $\tau < \tau(0) \approx -0.4028$ when $\alpha = 1000$ (for the other two cases $\tau(0) < -1$ and therefore $z > 0$ in the figure). We observe that the expansion is also accurate for negative z . As expected, the expansions fail close to the turning points ($\tau = 0, \tau = 1$).

We notice that, as is well know, the Laguerre polynomials $L_n^{(\alpha)}(uz)$ have n positive real zeros when $\alpha > -1$ and most of them in the interval (z_1, z_2) . Of course, the relative error (6.9) at the zeros is meaningless, and loss of relative accuracy is unavoidable very close to these zeros. In the previous figures, this loss of accuracy is not clearly revealed because the function is sampled at values of z which are not too close to the zeros (the sample values are not selected to avoid the zeros, simply happen to be not too close). Values of z very close to the zeros are needed to observe a significant accuracy loss; however, the

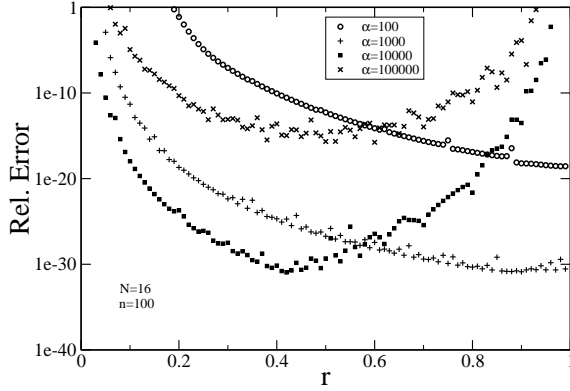


Fig. 9: The maximum relative error of the Airy expansion (6.2), with coefficients computed from (6.3) and (6.4), over the circles given by $z = z_2 + rr_m e^{i\theta}$, $\theta \in [0, 2\pi)$, $r_m = \min\{z_1, z_2 - z_1\}$, is plotted as a function of $r \in [0, 1]$.

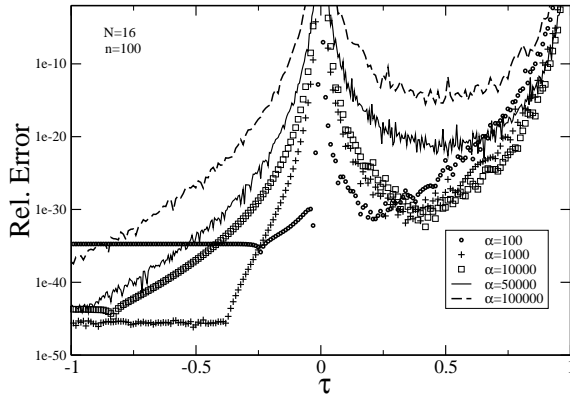


Fig. 10: Relative error ϵ_{rel} of the Airy expansion (6.2), with coefficients computed from (6.3) and (6.4), for real values of z as a function of $\tau = (z - z_1)/(z_2 - z_1)$.

previous plots show some effect of the zeros because the relative error gives a relatively noisy plot for values of z where zeros occur when compared to the cases without zeros. Compare, for example, the positive values of τ (for which there are zeros) with the negative values (no zeros) in Fig. 10. When we discuss Case 2 in the next section, we will show a detailed example of computation close to the zeros.

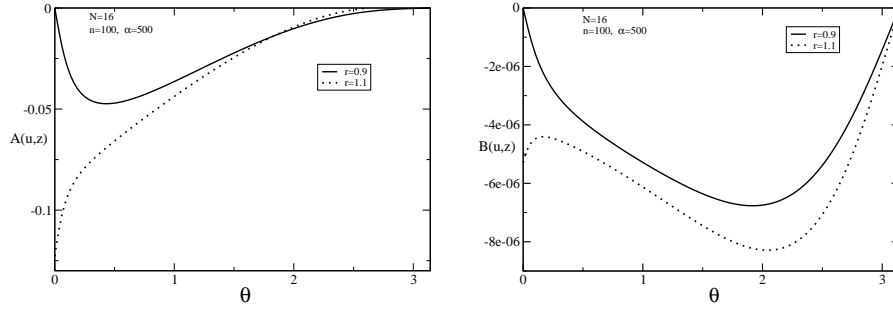


Fig. 11: Imaginary parts of the coefficient function approximations $\mathcal{A}_{N/2}(u, z)$ and $\mathcal{B}_{N/2}(u, z)$ as a function of θ , where $z = z_1 - rz_1 e^{-i\theta}$ for two values of r .

As commented before, even when the expansions are valid for $\operatorname{Re} z < 0$, these values can not be used for computing the coefficients by means of Cauchy integrals, due to the discontinuity at the branch cut. Fig. 11 shows this: we plot the imaginary part of the approximations $\mathcal{A}_m(u, z)$ and $\mathcal{B}_m(u, z)$ as functions of the angle when the radius is such that the circle cuts the negative real axis ($r = 1.1$), and when it does not ($r = 0.9$). For the second case, both coefficients are real over the real line, but not in the first case, when they have a non-zero imaginary part when z is real and negative, that is, when $\theta = 0$ (we move along the circles clockwise).

Finally, we notice that the relative error close to the turning point becomes large, as shown in Fig. 10; this indicates that, as expected, the L-G expansions for the coefficients of the Airy expansion are not accurate close to the turning point. This loss of accuracy is repaired by computing these coefficients by Cauchy integrals over a contour encircling the turning point (but sufficiently away from it) and contained in the half-plane $\operatorname{Re} z > 0$. Typically, the error that can be obtained around the turning point is close to the minimum error in Fig. 9 (choosing as Cauchy contour a circle with the radius corresponding to the minimum value of the error reached in that figure).

We give more explicit examples on the application of Cauchy integrals for the Case 2 asymptotics we discuss next.

6.2 Case 2

Now we provide numerical evidence of the accuracy of the expansions for Laguerre polynomials in domains containing the turning point z_2 .

From (5.11) the L-G approximation with N terms is now given by

$$L_n^{(\alpha)}(uz) = \frac{(-1)^n u^{(u-1)/2} (u+\alpha)^{(u+\alpha)/2}}{e^{u+(\alpha/2)} n! (uz)^{\alpha/2} \{(z-z_1)(z-z_2)\}^{1/4}} \times \exp \left\{ \frac{1}{2} uz - u\tilde{\xi} + \sum_{s=1}^N (-1)^s \frac{\hat{E}_s(z) - \lambda_s}{u^s} \right\} \left\{ 1 + \mathcal{O}\left(\frac{1}{u^{N+1}}\right) \right\}. \quad (6.10)$$

The order term is uniformly valid for $z \in \tilde{D}_2^+ \cup \tilde{D}_2^-$, where \tilde{D}_2^+ is shown in Fig. 5, and \tilde{D}_2^- is the conjugate region of \tilde{D}_2^+ .

The Airy expansion is given by (3.11), (5.13) and (5.14), uniformly for $z \in \tilde{\mathbf{D}}$ (the domain of validity depicted in Fig. 6). Hence truncating similarly to (6.2) - (6.4) we have

$$L_n^{(\alpha)}(uz) = \frac{(-1)^n 2\pi^{1/2} u^{(u/2)-(1/3)} (u+\alpha)^{(u+\alpha)/2}}{n! (uz)^{\alpha/2}} \times \exp \left\{ \frac{1}{2} uz - u - \frac{1}{2} \alpha + \sum_{s=0}^{m-1} \frac{\lambda_{2s+1}}{u^{2s+1}} \right\} \times \left[\text{Ai} \left(u^{2/3} \tilde{\zeta} \right) \left\{ \tilde{\mathcal{A}}_m(u, z) + \mathcal{O}\left(\frac{1}{u^{2m+1}}\right) \right\} + \text{Ai}' \left(u^{2/3} \tilde{\zeta} \right) \left\{ \tilde{\mathcal{B}}_m(u, z) + \mathcal{O}\left(\frac{1}{u^{2m+4/3}}\right) \right\} \right], \quad (6.11)$$

where, for any positive integer m ,

$$\tilde{\mathcal{A}}_m(u, z) = \tilde{\chi}(u, z) \exp \left\{ \sum_{s=1}^m \frac{\hat{E}_{2s}(z) + \tilde{a}_{2s} \tilde{\xi}^{-2s} / (2s)}{u^{2s}} \right\} \times \cosh \left\{ \sum_{s=0}^{m-1} \frac{\hat{E}_{2s+1}(z) - \tilde{a}_{2s+1} \tilde{\xi}^{-2s-1} / (2s+1)}{u^{2s+1}} \right\}, \quad (6.12)$$

and

$$\tilde{\mathcal{B}}_m(u, z) = \frac{\tilde{\chi}(u, z)}{u^{1/3} \tilde{\zeta}^{1/2}} \exp \left\{ \sum_{s=1}^m \frac{\hat{E}_{2s}(z) + a_{2s} \tilde{\xi}^{-2s} / (2s)}{u^{2s}} \right\} \times \sinh \left\{ \sum_{s=0}^{m-1} \frac{\hat{E}_{2s+1}(z) - a_{2s+1} \tilde{\xi}^{-2s-1} / (2s+1)}{u^{2s+1}} \right\}, \quad (6.13)$$

in which $\tilde{\chi}(u, z) = \left\{ \frac{\tilde{\zeta}}{(z-z_1)(z-z_2)} \right\}^{1/4}$.

As in Case 1a, if z is close to the turning point (this time z_2) we can replace $\tilde{\mathcal{A}}_m(u, z)$ by $(2\pi i)^{-1} \oint_{\mathcal{L}_2} \tilde{\mathcal{A}}_m(u, t) (t-z)^{-1} dt$ in (6.11), and similarly for $\tilde{\mathcal{B}}_m(u, z)$. Here \mathcal{L}_2 is a bounded contour in the t -plane that is positively orientated, lies in an equivalent domain to $\tilde{\mathbf{D}}$, and surrounds $t = z$ and $t = z_2$. As in Case 1a we typically take this to be a circle.

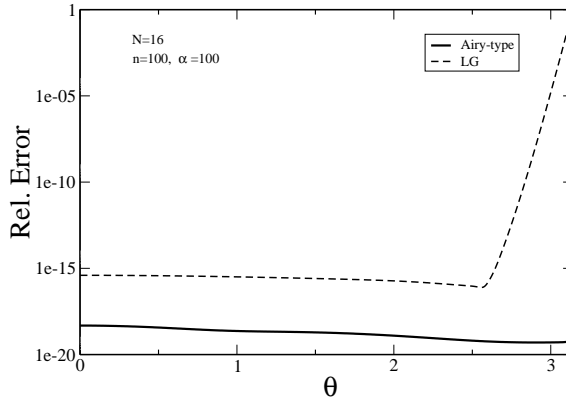


Fig. 12: Relative errors ϵ_{rel} for the L-G expansion (6.10) and the Airy (6.11) expansion, with coefficients computed from (6.12) and (6.13), as a function of θ , where $z = z_2 + Re^{i\theta}$, $\theta \in [0, \pi]$ and $R = 0.25(z_2 - z_1)$.

Figs. 12 and 13 compare the accuracy attainable for the L-G expansion (6.10) and the Airy expansion (6.11) - (6.13), both for real and complex variables. Figs. 14 and 15 illustrate the accuracy of this same Airy expansion but for different values of α . And, finally, Fig. 16 shows the accuracy of the Airy expansion with the coefficients computed by Cauchy integrals. In all of these cases, the coefficients of the Airy expansion are computed using $N = 16$ ($m = 8$), and the degree of Laguerre polynomials is set to $n = 100$.

In Fig. 12, we compare the L-G expansion with the Airy expansion away from the turning point (with coefficient functions still computed with (6.12) and (6.13)). The relative accuracy over a circle of radius $R = 0.25(z_2 - z_1)$ centered at z_2 is shown as a function of the angle $\theta \in [0, \pi]$; this half-circle is circulated counterclockwise. We observe that the L-G expansion (6.10) tends to fail for large θ in this interval, as the expansion loses meaning when we cross a Stokes line. Contrarily, the Airy type expansion (6.11) - (6.13) is valid in all the interval. In addition, we observe that the relative error for the Airy expansion is smaller than for the L-G expansion for all θ . We further explore this fact for real variables $z > z_2$ in Fig. 13.

Fig. 14 shows the maximum relative error of the Airy expansion (6.11) - (6.13), over circles centred at z_2 . As expected, the relative error increases both when the radius is small (because we are too close to the turning point z_2) as well as when part of the circle becomes too close to z_1 .

Fig. 15 shows again the relative error of the Airy expansion (6.11) - (6.13) with coefficients computed with asymptotic series, but for real variable. Again, the relative error increases close to the turning points. For $z > z_2$ the relative error decreases as z increases, as can be expected. This figure shows that our

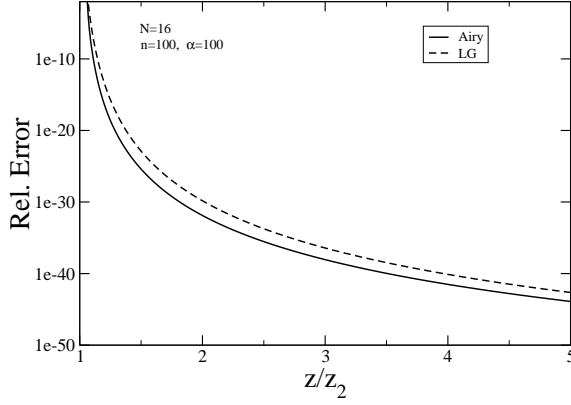


Fig. 13: Relative errors ϵ_{rel} for the L-G expansion (6.10) and the Airy expansion (6.11), with coefficients computed from (6.12) and (6.13), as a function of z/z_2 for real values of z , $z > z_2$.

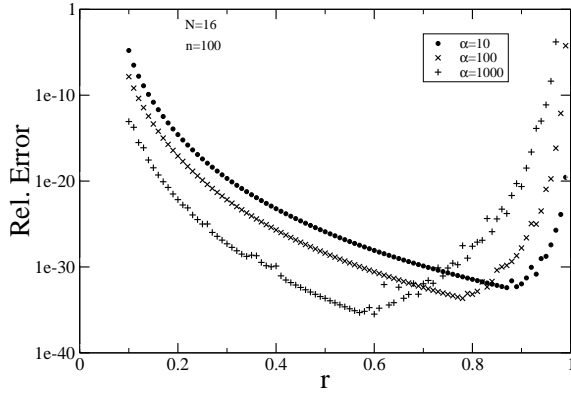


Fig. 14: The maximum relative error of the Airy expansion (6.11), with coefficients computed from (6.12) and (6.13), over the circles given by $z = z_2 + Re^{i\theta}$, $\theta \in [0, 2\pi)$ is plotted as a function of $r = R/(z_2 - z_1)$. The circles are sampled with 100 points.

alternative Cauchy integral method for the computation of the coefficients $\tilde{\mathcal{A}}_m(u, z)$ and $\tilde{\mathcal{B}}_m(u, z)$ is needed around the turning point.

Fig. 16 provides this computation using the trapezoidal rule with a discretization of 100 points in the upper half of the Cauchy contour (in the lower half we consider complex conjugation). Combining this computation with the

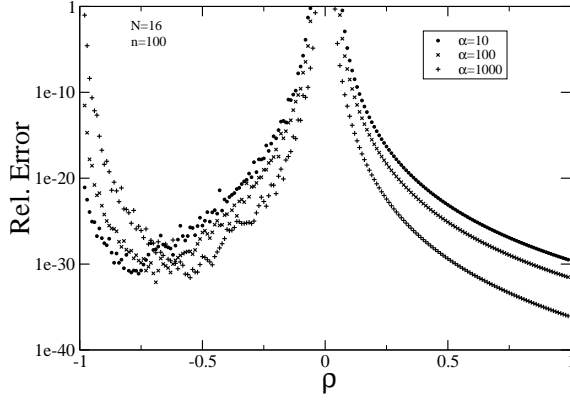


Fig. 15: Relative error ϵ_{rel} of the Airy expansion (6.11), with coefficients computed from (6.12) and (6.13), for real values of z as a function of $\rho = (z - z_2) / (z_2 - z_1)$.

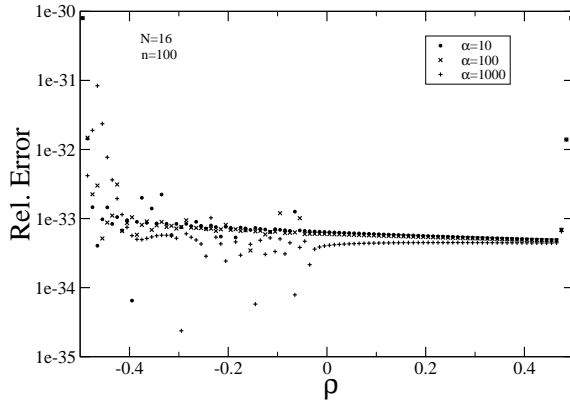


Fig. 16: Relative error ϵ_{rel} of the Airy expansion (6.11) for real values of z as a function of $\rho = (z - z_2) / (z_2 - z_1)$, with the coefficient approximations $\tilde{\mathcal{A}}_m(u, z)$ and $\tilde{\mathcal{B}}_m(u, z)$ computed by Cauchy integrals. The Cauchy contour is a circle of radius $R = 0.7(z_2 - z_1)$ centred at z_2 .

results in Fig. 15 we observe that it is possible to compute accurately the Laguerre polynomials for $z > z_1$, but not too close to z_1 .

Observe that, according to Fig. 14 (see also Fig. 15), over a circle of radius $0.7(z_2 - z_1)$ centered at z_2 , the relative errors are of the order of 10^{-30} , and we observe that the application of Cauchy integrals permits us to maintain this accuracy inside the circle (but not too close to the circle). As we see in Fig.

16, the relative error has little variation and it is of the order of 10^{-30} inside the circle $|z - z_2| < 0.5(z_2 - z_1)$ (the figure is only for real z but the same is true for complex z).

As we commented in the previous subsection, the *relative* accuracy unavoidably degrades very close to the zeros and this degradation is, for example, responsible for the different appearance of the graphs for $\rho > 0$ and $\rho < 0$ in Figs. 15 and 16.

To illustrate the uniform accuracy of our approximations near the zeros we need to replace the denominator of (6.9) with an "envelope" of the Laguerre polynomial, which mimics the amplitude of $L_n^{(\alpha)}(x)$ but does not vanish at its zeros. For polynomials having simple zeros, the envelope function $\text{env}f(x) = \{f^2(x) + f'^2(x)\}^{1/2}$ serves this purpose. Then we define the modified relative error of an approximation f^* to a function f as

$$\hat{\epsilon}_{rel} = \frac{|f - f^*|}{\text{env}f}, \quad (6.14)$$

where in our case $f(x) = L_n^{(\alpha)}(x)$.

In Fig. 17 we then show similar results for the Airy expansion in a more restricted interval containing two zeros. In this both the relative error ϵ_{rel} (solid line) and the modified relative error $\hat{\epsilon}_{rel}$ (dashed line) are shown. In the figure we used many more sample points than in Fig. 16, so that the (unavoidable) degradation of the relative error ϵ_{rel} becomes more apparent, whereas in contrast the modified relative error $\hat{\epsilon}_{rel}$ remains bounded. As can be seen, the degradation of ϵ_{rel} only takes place very close to the zeros. Of course, this *relative* error degradation is unavoidable and common to any method of numerical computation. On the other hand, $\hat{\epsilon}_{rel}$ is small throughout the interval which illustrates the uniform *absolute* accuracy of our Airy expansion in the whole interval.

Finally, we give some additional results for other values of n , α and N as a further illustration of the accuracy of the computation using Cauchy integrals. We pick a value of z in the disc $|z - z_2| < 0.5(z_2 - z_1)$. In particular, we fix $z = z_1 + 0.1(z_2 - z_1)$. We show the corresponding relative errors in Table 1. In the table, we take 300 points in the upper half of the Cauchy contour because with the previous selection (100 points) the discretization error is not small enough in some cases; in particular for $n = 1000$ and $N = 16$ ($m = N/2 = 8$), when the relative error becomes of the order of 10^{-50} .

We observe in Table 1 that the relative error shows little variation with the value of α , as the previous figures also showed, and that the dependence on n and N is as expected for asymptotic approximations with an error of $\mathcal{O}(n^{-N-1})$.

This is shown more explicitly in Table 2, where we give the values of the computational asymptotic error constants $n^{N+1}\epsilon_{rel}$, with ϵ_{rel} the relative errors in Table 1; we observe these experimental constants have a slow variation as a function of n and α . While we also expect these constants to be $\mathcal{O}(1)$

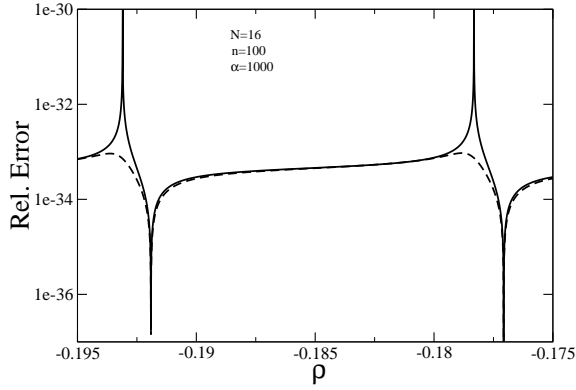


Fig. 17: Relative error ϵ_{rel} (solid line) and modified relative error $\hat{\epsilon}_{rel}$ (dashed line) of the Airy expansion (6.11) for real values of z as a function of $\rho = (z - z_2) / (z_2 - z_1)$, with the coefficient approximations $\tilde{\mathcal{A}}_m(u, z)$ and $\tilde{\mathcal{B}}_m(u, z)$ computed by Cauchy integrals. The Cauchy contour is a circle of radius $R = 0.7(z_2 - z_1)$ centered at z_2 .

$N \Rightarrow$ α, n \Downarrow	2	4	8	12	16
0, 10	$1.15 \cdot 10^{-6}$	$2.88 \cdot 10^{-9}$	$2.20 \cdot 10^{-13}$	$1.28 \cdot 10^{-16}$	$2.86 \cdot 10^{-19}$
0, 100	$1.46 \cdot 10^{-9}$	$4.03 \cdot 10^{-14}$	$3.65 \cdot 10^{-22}$	$2.45 \cdot 10^{-29}$	$6.24 \cdot 10^{-36}$
0, 1000	$1.50 \cdot 10^{-12}$	$4.21 \cdot 10^{-19}$	$3.89 \cdot 10^{-31}$	$2.66 \cdot 10^{-42}$	$6.85 \cdot 10^{-53}$
100, 10	$4.90 \cdot 10^{-7}$	$1.22 \cdot 10^{-9}$	$9.53 \cdot 10^{-13}$	$5.68 \cdot 10^{-17}$	$1.30 \cdot 10^{-19}$
100, 100	$7.79 \cdot 10^{-10}$	$1.94 \cdot 10^{-14}$	$1.69 \cdot 10^{-22}$	$1.13 \cdot 10^{-29}$	$2.88 \cdot 10^{-36}$
100, 1000	$1.31 \cdot 10^{-12}$	$3.41 \cdot 10^{-19}$	$2.76 \cdot 10^{-31}$	$1.70 \cdot 10^{-42}$	$4.06 \cdot 10^{-53}$

Table 1: Relative error ϵ_{rel} of the Airy expansion (6.11) with $z = z_2 + 0.1(z_2 - z_1)$, where the coefficient approximations $\tilde{\mathcal{A}}_m(u, z)$ and $\tilde{\mathcal{B}}_m(u, z)$ are computed by Cauchy integrals over the contour $|z - z_2| = 0.7|z_2 - z_1|$; different selections of the degree n , the parameter α and the number of coefficients in the asymptotic expansion $N = 2m$ are considered.

$N \Rightarrow$ α, n \downarrow	2	4	8	12	16
0, 10	$1.15 \cdot 10^{-3}$	$2.88 \cdot 10^{-4}$	$2.20 \cdot 10^{-4}$	$1.28 \cdot 10^{-3}$	$2.86 \cdot 10^{-2}$
0, 100	$1.46 \cdot 10^{-3}$	$4.03 \cdot 10^{-4}$	$3.65 \cdot 10^{-4}$	$2.45 \cdot 10^{-3}$	$6.24 \cdot 10^{-2}$
0, 1000	$1.50 \cdot 10^{-3}$	$4.21 \cdot 10^{-4}$	$3.89 \cdot 10^{-4}$	$2.66 \cdot 10^{-3}$	$6.85 \cdot 10^{-2}$
100, 10	$4.90 \cdot 10^{-4}$	$1.22 \cdot 10^{-4}$	$9.53 \cdot 10^{-5}$	$5.68 \cdot 10^{-4}$	$1.30 \cdot 10^{-2}$
100, 100	$7.79 \cdot 10^{-4}$	$1.94 \cdot 10^{-4}$	$1.69 \cdot 10^{-4}$	$1.13 \cdot 10^{-3}$	$2.88 \cdot 10^{-2}$
100, 1000	$1.31 \cdot 10^{-3}$	$3.41 \cdot 10^{-4}$	$2.76 \cdot 10^{-4}$	$1.70 \cdot 10^{-3}$	$4.06 \cdot 10^{-2}$

Table 2: Computational asymptotic error constants estimated from the errors of Table 1.

they are in fact all quite small, which illustrates the uniform high accuracy of our Airy expansions.

References

1. Dunster, T.M.: Uniform asymptotic expansions for Whittaker’s confluent hypergeometric functions. *SIAM J. Math. Anal.* **20**(3), 744–760 (1989). DOI 10.1137/0520052. URL <http://dx.doi.org/10.1137/0520052>
2. Dunster, T.M.: Asymptotics of the eigenvalues of the rotating harmonic oscillator. *J. Comput. Appl. Math.* **93**(1), 45–73 (1998). DOI 10.1016/S0377-0427(98)00070-3. URL [http://dx.doi.org/10.1016/S0377-0427\(98\)00070-3](http://dx.doi.org/10.1016/S0377-0427(98)00070-3)
3. Dunster, T.M., Gil, A., Segura, J.: Computation of asymptotic expansions of turning point problems via Cauchy’s integral formula: Bessel functions. *Constructive Approximation* pp. 1–31 (2017). DOI 10.1007/s00365-017-9372-8. URL <http://dx.doi.org/10.1007/s00365-017-9372-8>
4. Farid Khwaja, S., Olde Daalhuis, A.B.: Computation of the coefficients appearing in the uniform asymptotic expansions of integrals. *Studies in Applied Mathematics* (2017). DOI 10.1111/sapm.12172. URL <http://dx.doi.org/10.1111/sapm.12172>
5. Frenzen, C.L., Wong, R.: Uniform asymptotic expansions of Laguerre polynomials. *SIAM J. Math. Anal.* **19**(5), 1232–1248 (1988). DOI 10.1137/0519087. URL <http://dx.doi.org/10.1137/0519087>
6. Gil, A., Segura, J., Temme, N.M.: Efficient computation of Laguerre polynomials. *Comput. Phys. Commun.* **210**, 124–131 (2017). DOI 10.1016/j.cpc.2016.09.002. URL <http://dx.doi.org/10.1016/j.cpc.2016.09.002>
7. Olde Daalhuis, A.B.: Confluent hypergeometric functions. In: *NIST handbook of mathematical functions*, pp. 321–349. U.S. Dept. Commerce, Washington, DC (2010)
8. Olver, F.W.J.: Whittaker functions with both parameters large: uniform approximations in terms of parabolic cylinder functions. *Proc. Roy. Soc. Edinburgh Sect. A* **86**(3-4), 213–234 (1980). DOI 10.1017/S0308210500012130. URL <http://dx.doi.org/10.1017/S0308210500012130>
9. Olver, F.W.J.: Asymptotics and special functions. *AKP Classics*. A K Peters Ltd., Wellesley, MA (1997). Reprint of the 1974 original [Academic Press, New York]
10. Olver, F.W.J.: Airy and related functions. In: *NIST handbook of mathematical functions*, pp. 193–213. U.S. Dept. Commerce, Washington, DC (2010)

-
11. Temme, N.M.: Asymptotic estimates for Laguerre polynomials. *Z. Angew. Math. Phys.* **41**(1), 114–126 (1990). DOI 10.1007/BF00946078. URL <http://dx.doi.org/10.1007/BF00946078>
 12. Temme, N.M.: Asymptotic methods for integrals, *Series in Analysis*, vol. 6. World Scientific Publishing Co. Pte. Ltd., Hackensack, NJ (2015)